Dielectric properties of single-crystal $TiSi_2$ from 0.6 to 20 eV

M. Tanaka and S. Kurita
Laboratory of Applied Physics, Faculty of Engineering, Yokohama National University, Yokohama 240, Japan

M. Fujisawa
Synchrotron Radiation Laboratory, Institute for Solid State Physics, University of Tokyo, Tokyo 188, Japan

F. Lévy
Institut de Physique Appliquée, Ecole Polytechnique Fédérale de Lausanne, 1015 Lausanne, Switzerland

(Received 12 September 1990)

The electronic structure of $TiSi_2$ has been examined by measuring polarized reflectivity spectra of single crystals in the photon-energy range from 0.6 to 20 eV. The complex dielectric functions and the optical conductivities are determined by Kramers-Kronig analysis. The spectral structures are discussed in terms of interband transitions among Ti 3*d* states and Si 3*s*-3*p* states with the aid of published results of band-structure calculations. The effective number of electrons contributing to optical transitions and the electron-energy-loss functions are also calculated and discussed.

INTRODUCTION

Refractory-metal (group-IVA, -VA, and -VIA) disilicides have been extensively studied in connection with applications in very-large-scale-integration (VLSI) technology, such as interconnects, gate metallization, and Schottky barriers. This is because they have high electrical conductivity and good thermal and chemical stability, and are compatible with conventional polysilicon microfabrication processes.[1] $TiSi_2$ has the highest conductivity within the metal silicide family and is one of the most promising candidates for use as a contact and interconnect material. The main concern has been focused on the condition of thin-film formation and characterization. Detailed studies on their physical properties, however, have been lacking.

The electronic structure of the valence and conduction bands of $TiSi_2$ has been studied by optical spectroscopy,[2-4] electron spectroscopy,[5-8] and band calculations.[6,8,9] The optical data are limited to the photon-energy range below 8 eV. Unpolarized reflectivity (R) spectra of single crystal have been reported, and the low- and high-energy parts have been discussed on the basis of the Drude model and the existing band-structure information, respectively.[4] X-ray photoemission (XPS) and bremsstrahlung isochromat spectra (BIS) of systematically chosen transition-metal disilicides have been well described by the calculated spectra including matrix elements as well as the density of states (DOS).[8] A detailed band-structure calculation of $TiSi_2$ has been presented and the projected Ti 3*d* DOS has been shown to agree with the published ultraviolet photoemission spectra (UPS).[9] The overall band structure and features originating mainly from Ti 3*d* states and Si 3*s*-3*p* states are now generally accepted. Therefore, an optical spectroscopic study in the vacuum-ultraviolet (vuv) range, especially above 8 eV, is desirable at this time for a detailed examination of the electronic structure. Optical spectroscopy has higher resolution than electron spectroscopy, while providing complementary information.

Single crystals are indispensable for a precise study of the physical properties of ordered solids in order to eliminate ambiguities common to polycrystalline films and samples arising from composition fluctuation, structural inhomogeneity, and surface roughness. Specifically, surface roughness severely reduces reflectivity in the ultraviolet (uv) range.[10] Even if single crystals are used, there is still the ever present problem of surface oxidation. Surfaces of as-grown crystals are more or less covered by oxide layers, and these overlayers can also reduce the reflectivity in the uv range. Some surface treatment is thus necessary for reliable optical measurements in the uv range.

In this paper, polarized reflectivity (R) spectra of single-crystal $TiSi_2$ in the photon-energy range up to 20 eV are presented. Chemical etching was performed before every measurement to remove oxide overlayers. The R data are converted by Kramers-Kronig (KK) analysis into complex dielectric functions ($\bar{\epsilon}$) and optical conductivities ($\sigma_{\rm opt}$). The spectral structures of $\sigma_{\rm opt}$ are attributed to interband transitions corresponding to the DOS features of the published energy bands.[9] The effective number of electrons contributing to optical transitions ($n_{\rm eff}$) and the electron-energy-loss function $-\mathrm{Im}(1/\bar{\epsilon})$ are also obtained from $\bar{\epsilon}$. Plasmon energies are compared with published results obtained with electron-energy-loss spectroscopy.

EXPERIMENT

Single-crystalline samples were prepared in the vapor phase by chemical transport reactions. Reacted titanium

silicide (5–10 g) was degassed in the reaction quartz crucibles (35 mm in diameter and 200 mm in length). The transport agent I_2 was added from an enclosed soft-glass ampoule in the already sealed crucible. The temperature of the charge was between 1090 °C and 1120 °C, whereas the growth temperature was between 1060 °C and 1080 °C. Small temperature differences between the charge and growth zones improved the growth conditions and large crystals—platelike or needlelike—have been obtained after 4–6 weeks. A typical dimension of the sample surface used in the measurements was 2.5×8 mm^2. The crystal structure of some samples has been checked by x-ray powder-diffraction analysis. It is the face-centered orthorhombic $C54$-type structures [space group D_{2h}^{24} ($Fddd$)]. The lattice parameters are $a=8.253$ Å, $b=4.783$ Å, and $c=8.540$ Å.[11] The orientation of the sample was determined by x-ray diffraction patterns.

The R spectra were measured at room temperature in two different systems, depending on the photon-energy range. In the vuv range from 3 to 20 eV, the R spectra were measured with a 0.4-GeV electron-storage ring at Synchrotron Radiation Laboratory, Institute for Solid State Physics, University of Tokyo. Linearly polarized light monochromatized by a 1-m focal-length Seya-Namioka-type monochromator with a resolution of about 0.3 nm was incident on the surface of the crystal. The angle of incidence was about 20°. The reflected light was detected by photomultipliers with a coating of sodium salicylate for 6–20 eV and without coating for 3–6 eV. The signal was always normalized by the total light intensity, which was monitored by the photoemission current from a Au mesh plate at the entrance of the monochromator. The R spectra are calculated after measurement as the ratio of this normalized spectra of reflection to the normalized spectra of the incident light.

The double-beam system was used in the photon-energy range from 0.6 to 4.0 eV. Light emerging from the monochromator was polarized with a Glan-Thompson prism and split into two beams by a thin quartz plate. One beam hit the surface of the crystal at normal incidence and the other beam was directed to an Al mirror whose reflectivity was measured in advance. After reflection on the crystal and the reference mirror, the beams were brought into coincidence on the quartz beam splitter. The signal detected by a photomultiplier or a PbS photodiode was fed into two lock-in amplifiers and the measurements were collected by a microcomputer. The absolute values of the reflectivity were determined at 2.41 eV using an Ar^+ laser and a photometer.

Refractory-metal disilicides are easily oxidized. The reflectivities of the as-grown crystal and the crystal exposed in air for some time were found to be substantially suppressed in the vuv range relative to that of the chemically etched one. On the other hand, over-etching produced surface roughness which also reduces the reflectivity in the vuv range. Therefore, specimens were carefully etched by HF and HNO_3 solution just before every measurement. Spectral features and polarization dependence were only slightly affected by the etching. The relative accuracies of the obtained reflectivity were about ±5% in the range below 4 eV and about ±10% in the vuv range. These inaccuracies were mainly dominated by the imperfect reproducibility of the surface treatment.

RESULTS

The R spectra are shown in Fig. 1. The solid and dashed curves correspond to spectra for light polarized parallel to the a axis ([100]) and b axis ([010]), as indicated by $\mathbf{E}\|a$ and $\mathbf{E}\|b$, respectively. In each spectrum, a sharp cutoff occurs at around 1 eV and is followed by some small features in the visible (vis) range, a massive peak around 6.5 eV, a shoulder at 10.6 eV, and a broad hump around 15 eV. In the vis range, the R spectra reveal anisotropic features. The $\mathbf{E}\|a$ spectrum has two small peaks at 1.31 and 1.98 eV, whereas the $\mathbf{E}\|b$ spectrum does not have a significant structure. The unpolarized R spectrum of $TiSi_2$ single crystal has been published in the range from 0.01 to 7.7 eV.[4] An average of our $\mathbf{E}\|a$ and $\mathbf{E}\|b$ spectra agrees with their spectrum within experimental error in the range from 0.6 to 7 eV.

The complex dielectric function $\bar{\epsilon}(\omega)=\epsilon_1(\omega)+i\epsilon_2(\omega)$ is more suitable than the R spectra for an interpretation of optical properties, such as electronic structures, from a microscopic point of view. The $\epsilon_1(\omega)$ and $\epsilon_2(\omega)$ spectra obtained by the KK analysis of the R spectra are shown in Fig. 2. In this analysis, the R spectra are extrapolated into the unmeasured range, that is, below 0.6 eV and above 20 eV. The published R data for unpolarized light[4] are used for the lower-photon-energy range. The suitability of the extrapolation is supported by the following reasons. Intraband transition due to free carriers mainly contributes to the high reflectivity in this range. The optical spectra are then well described by the Drude model with two parameters: the plasma frequency ω_p and the mean free time between scattering events, τ. These pa-

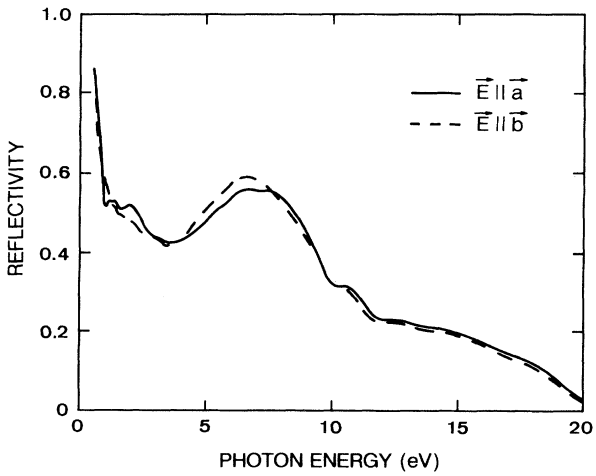

FIG. 1. Reflectivity spectra of $TiSi_2$ at room temperature. Solid and dashed curves correspond to the spectra for lights polarized parallel to the a axis ($\mathbf{E}\|a$) and the b axis ($\mathbf{E}\|b$), respectively.

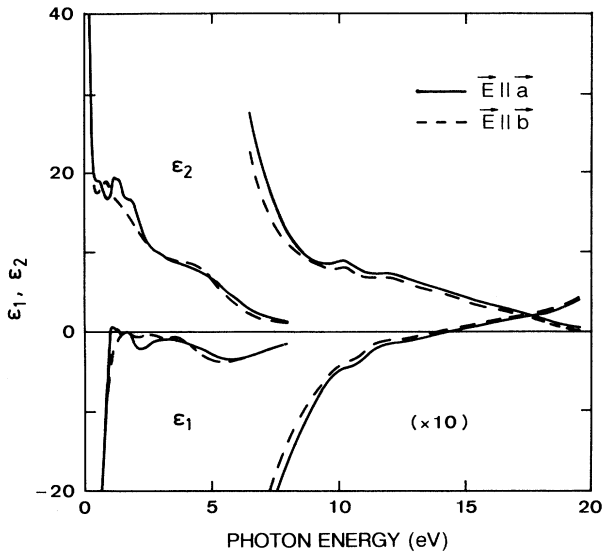

FIG. 2. Complex dielectric functions ($\bar{\epsilon}$) of $TiSi_2$. Upper and lower parts correspond to imaginary (ϵ_2) and real (ϵ_1) parts of $\bar{\epsilon}$, respectively. The spectra in the range above 7 eV are magnified by 10.

rameters are also estimated from the dc conductivity, $\sigma=\omega_p^2\tau/4\pi$. The anisotropy of the dc conductivity is known to be very small:[12] $\sigma([100])=0.91\times10^5$ $\Omega^{-1}\,\mathrm{cm}^{-1}$ and $\sigma([010])=1.00\times10^5$ $\Omega^{-1}\,\mathrm{cm}^{-1}$. Therefore, the anisotropy of reflectivity in the Drude range is also expected to be small, so that one may extrapolate the $\mathbf{E}\|a$ and $\mathbf{E}\|b$ spectra to give the same unpolarized spectrum. In the higher-photon-energy range, the R spectra are extrapolated by the conventional method; $R(E)=R(20\text{ eV})[(20\text{ eV})/E]^s$. The parameter s is adjusted so as to minimize the deviation between the calculated optical constants and the published data determined by ellipsometry at 1.960 eV: $(n,k)=(2.65, 2.14)$ for single crystal.[4] Since these data were measured with unpolarized light, the average of our data was compared with their data. The optimum s value was obtained as 4.9 which gives $\delta_n=\Delta n/n=0.38\times10^{-2}$, $\delta_k=\Delta k/k=2.41\times10^{-2}$, and $\delta=\sqrt{(\delta_n^2+\delta_k^2)/2}=1.7\times10^{-2}$.

The dashed and solid curves in Fig. 2 correspond to the $\mathbf{E}\|a$ and $\mathbf{E}\|b$ spectra, respectively. The right half of the spectra was magnified by 10 for improved visibility. The general features of the ϵ_2 spectra are similar to those of the R spectra, except that peaks at 4.65 and 12.5 eV appear in the ϵ_2 spectra instead of the peaks at 6.5 and 15 eV in the R spectra. The present optical data constitute three improvements over the earlier published data. First, the ϵ_2 data in the vuv range are determined; and moreover, surface treatments were performed to minimize the effect of oxide overlayers. Second, the anisotropy, which has not hitherto been available even in the visible range, is given. Third, availability of the R data over a wider range increases the accuracy of the KK transformation.

DISCUSSION

Overall, features of interband transitions are not easily seen in the $\bar{\epsilon}$ spectra, because the ϵ_2 value decreases by a factor of $1/\omega$ even if the oscillator strength and the joint density of states remain constant. The optical conductivity $\sigma_{\mathrm{opt}}=\omega\epsilon_2/4\pi$ shown in Fig. 3 is thus more suitable for an interpretation of the spectral structures in terms of interband transitions. Each σ_{opt} spectrum is dominated by a great peak extending in the range from 0.2 to 8 eV, followed by two small humps located at 10.3 and 12.2 eV. An anisotropy is definitely seen in the lower range: The $\mathbf{E}\|a$ spectrum has a peak at 1.97 eV, whereas the $\mathbf{E}\|b$ spectrum has only a shoulder there. On the other hand, the peak around 4.5 eV for the $\mathbf{E}\|a$ is smaller than that for the $\mathbf{E}\|b$. In Fig. 3, dotted curves represent the contribution of the interband transition which is obtained by subtracting the contribution of the intraband transition. The intraband contribution is estimated from the Drude model with $\hbar\omega_p=4.2$ eV and $\tau=4.5\times10^{-14}$ s.[4] The onset of the interband transition is thus found to occur at about 0.2 eV.

The band structures of $3d$ transition-metal disilicides from $TiSi_2$ to $NiSi_2$ were roughly estimated by UPS and calculations in the hypothetical crystal structures.[6] The XPS and BIS of $3d$, $4d$, and $5d$ transition-metal disilicides have been well reproduced by the calculations in the real crystal structures including matrix elements.[8] According to these results, the overall features of the valence and conduction bands are dominated by Si s and p states and metal d states. Most of the Si s states are concentrated at 8–10 eV below the Fermi level E_F, and partially contribute to the conduction bands. Due to a hybridization between the Si p and the metal d states, they contribute the large peaks in the DOS below and above E_F. The metal d states are distributed in a narrower range, about 6 eV below and above E_F, than the Si

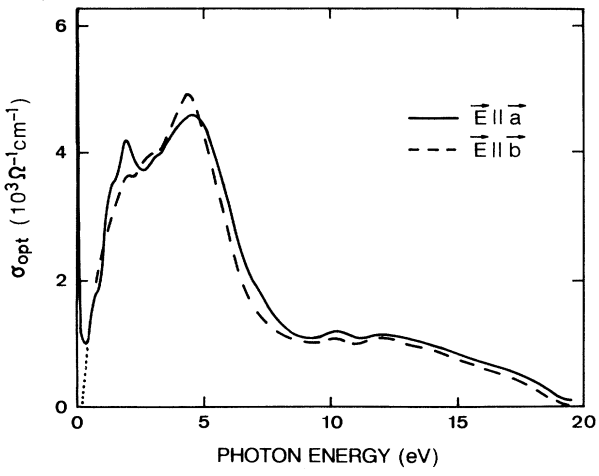

FIG. 3. Optical conductivities of $TiSi_2$. Dotted curves in the lower energy range show the interband contribution which is obtained by subtracting the Drude term due to intraband transition.

p states. The states originating mostly from the metal d states are situated in between the bonding and antibonding states of the p-d-hybridized states. The center of these mostly d states moves across E_F from above to below as the number of metal d electrons increases from Ti to Ni.

In early-transition-metal disilicides such as $TiSi_2$, the bandwidth of the mostly d states is generally larger and their contribution to the DOS is less prominent compared with the late-transition-metal disilicides, and the distribution of the metal d states extends more in the conduction bands than the valence bands.[8] The dispersion of the energy bands in the Brillouin zone of $TiSi_2$ has been presented, and the Ti $3d$ DOS is shown to agree well with the published UPS.[9] Unfortunately, the BIS of $TiSi_2$ has not been reported yet, so that information about the conduction band is limited. From the energy bands in Fig. 4 in Ref. 9, onset of interband transitions seems to occur at the B point in the Brillouin zone where the band gap is about 0.3 eV. This agrees well with the onset seen in Fig. 3. Even if this transition is forbidden, there are some points around the B point where interband transitions occur below 0.5 eV. However, the symmetry of bands, which is not available in Ref. 9, should be taken into account before making definite assignments. Meanwhile, the DOS curves from 13 eV below E_F to 5 eV above E_F are shown in Fig. 5 in Ref. 9. According to the DOS, the Ti $3d$ component exhibits a modest peak at 1.0 eV (V_1) below E_F and dominates the conduction-band feature including three peaks at 1.1 eV (C_1), 2.8 eV (C_2), and 4.2 eV (C_3) above E_F, whereas the Si component is essentially featureless but provides relatively large contributions to V_1 and C_3. Therefore, V_1 and C_3 can be interpreted to originate mainly from the bonding and antibonding states of the p-d-hybridized states, respectively, whereas C_1 and C_2 originate from the mostly Ti $3d$ states.

Comparing the energies of the structures in the σ_{opt} spectra with those of the DOS peaks in Ref. 9, we attribute the peak at 1.97 eV for $\mathbf{E}\|a$ and the shoulder at 1.98 eV for $\mathbf{E}\|b$ to the $V_1 \rightarrow C_1$ transition (2.1 eV), and the peak at 4.57 eV for $\mathbf{E}\|a$ and the peak at 4.36 eV for $\mathbf{E}\|b$ to an overlap of the two transitions $V_1 \rightarrow C_2$ (3.8 eV) and $V_1 \rightarrow C_3$ (5.2 eV). On the other hand, the spectral structures above 8 eV cannot be fully discussed because of the lack of the DOS of the higher conduction bands. However, it is probable that they are partially related to the Si s states concentrated at about 10 eV below E_F as well as the Ti d and Si p states. Judging only from the existing information, we could tentatively attribute the small humps located at 10.3 and 12.2 eV to the transitions from the Si s states to C_1 and C_2, because the energy difference between C_1 and C_2 (1.7 eV) is close to that between the spectral structures (1.9 eV) and both C_1 and C_2 are mainly from Ti $3d$ states. Further detailed assignment of the spectral structures should be left for a calculation including both the joint density of states and transition probability.

The effective number of electrons per molecule contributing to the optical properties over a finite frequency range, $n_{\text{eff}}(\omega)$, is obtained from the finite-energy oscillator strength (f) sum rules:[13]

$$n_{\text{eff}}(\omega)=\frac{m}{2\pi^2 Ne^2}\int_0^{\omega}\omega'\epsilon_2(\omega')d\omega' ,$$

where N is the density of molecules, 2.37×10^{22} molecules/cm^3, and m and e are the mass and the charge of an electron. Figure 4 shows the n_{eff} spectra for $\mathbf{E}\|a$ and $\mathbf{E}\|b$ polarization. Contribution at zero frequency is estimated from $\sigma_{\text{opt}}(0)=\omega_p^2\tau/4\pi=1.6\times10^5\ \Omega^{-1}\,\text{cm}^{-1}$.[4] As is seen in Fig. 3, the spectral structures from 1 to 8 eV mainly contribute to the f sum rule. The n_{eff} spectra then gradually increase and reach about 5.5 electrons per molecule at 20 eV. Since $E=20$ eV almost exhausts the valence-electron oscillator strength and is far below the lowest core transitions from Ti $3p$ states (33 eV),[6] n_{eff}(20 eV) roughly corresponds to the number of valence electrons. Taking the $3d^2 4s^2$ configuration for Ti and the $3s^2 3p^2$ configuration for Si into account, one ends up with twelve as the number of valence electrons per molecule. Therefore, about half of the valence electrons contributes to the optical transitions below 20 eV. The

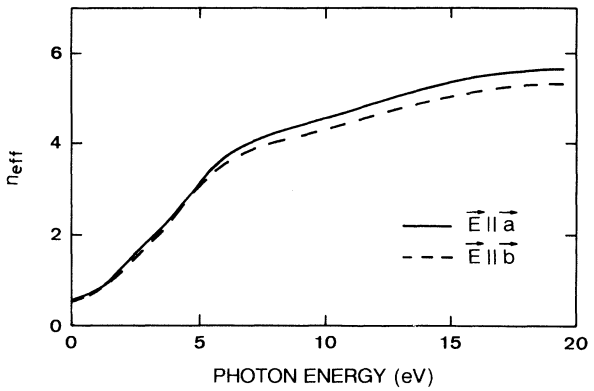

FIG. 4. Effective numbers of electrons contributing to optical transitions (n_{eff}) of $TiSi_2$.

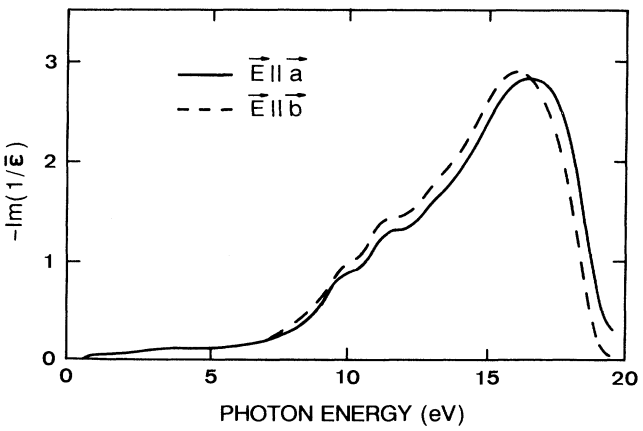

FIG. 5. Electron-energy-loss functions $-\text{Im}(1/\tilde{\epsilon})$ of $TiSi_2$.

above behavior of n_{eff} is often seen in transition metals with d electrons such as Ti.[14] The anisotropy in the n_{eff} spectra is noticeable over the whole range. An anisotropy in n_{eff} was also reported for other silicides, $MoSi_2$ and WSi_2, although they were evaluated in the limited range between 1.3 and 4.8 eV.[15]

The $\bar{\epsilon}$ spectra provide insight about not only one-electron band structures but also collective excitations of the electron gas, that is, plasmons. Plasmons are excited by an electron passing through a solid. The probability of energy loss by a fast electron is proportional to $-\text{Im}(1/\bar{\epsilon})$. Figure 5 shows the electron-energy-loss functions calculated from the $\bar{\epsilon}$ spectra in Fig. 2. Each spectrum is dominated by a strong peak at about 16.3 eV with two shoulders at 11.4 and 9.9 eV. Anisotropy is seen in the whole range, and the peak energies for the $\mathbf{E}\|a$ and $\mathbf{E}\|b$ are 16.5 and 16.1 eV, respectively. Peaks of a $-\text{Im}(1/\bar{\epsilon})$ spectrum are generally identified as due to volume plasmons, when ϵ_2 is small, $d\epsilon_1/d\omega > 0$, and $d\epsilon_2/d\omega < 0$.[16] Therefore, the peak around 16.3 eV in the $-\text{Im}(1/\bar{\epsilon})$ spectra is attributed to volume-plasmon excitations, whereas other structures are due to interband transitions. These plasmons correspond to the collective excitations of valence electrons. A published electron-energy-loss measurement of $TiSi_2$ film shows that there is a peak at 16.8 eV in the second energy derivative of the energy-loss function.[17] This peak was assigned as due to volume-plasmon excitation. The plasmon energies determined from the ϵ_2 data in the present investigation are in agreement with the published data on thin films. This agreement reinforces the advisability of the present analysis and the accuracy of the $\bar{\epsilon}$ data in the vuv range.

ACKNOWLEDGMENTS

H. Berger is acknowledged for the growth of the single crystal. Discussion with Dr. T. Koide was very beneficial.

[1]S. P. Murarka, J. Vac. Sci. Technol. **17**, 775 (1980).
[2]K. Lee and J. T. Lue, Phys. Lett. A **125**, 271 (1987).
[3]W. Henrion and H. Lange, Phys. Status Solidi B **151**, 375 (1989).
[4]A. Borghesi, A. Piaggi, G. Guizzetti, F. Lévy, M. Tanaka, and H. Fukutani, Phys. Rev. B **40**, 1611 (1989).
[5]A. Franciosi and J. H. Weaver, Surf. Sci. **132**, 324 (1983).
[6]J. H. Weaver, A. Franciosi, and V. L. Moruzzi, Phys. Rev. B **29**, 3293 (1984).
[7]G. Peto, E. Zsoldos, L. Guczi, and Z. Schay, Solid State Commun. **57**, 817 (1986).
[8]W. Speier, E. V. Leuken, J. C. Fuggle, D. D. Sarma, L. Kumar, B. Dauth, and K. H. J. Buschow, Phys. Rev. B **39**, 6008 (1989).
[9]L. F. Mattheiss and J. C. Hensel, Phys. Rev. B **39**, 7754 (1989).
[10]M. Tanaka, P. E. Schmid. A. Piaggi, and F. Lévy, J. Vac. Sci. Technol. A **7**, 3287 (1989).
[11]W. B. Pearson, *The Crystal Chemistry and Physics of Metals and Alloys* (Wiley-Interscience, New York, 1972).
[12]F. Nava, E. Mazzega, M. Michelini, O. Laborde, O. Thomas, J. P. Senateur, and R. Mader, J. Appl. Phys. **65**, 1584 (1989).
[13]D. Y. Smith, in *Handbook of Optical Constants of Solids,* edited by E. D. Palik (Academic, New York, 1985), Chap. 3.
[14]D. W. Lynch, C. G. Olson, and J. H. Weaver, Phys. Rev. B **11**, 3617 (1975).
[15]F. Ferrieu, C. Viguier, A. Cros, A. Humvert, O. Thomas, R. Madar, and J. P. Senateur, Solid State Commun. **62**, 455 (1987).
[16]J. H. Weaver, D. W. Lynch, and C. G. Olson, Phys. Rev. B **10**, 501 (1974).
[17]J. K. N. Sharma, B. R. Chakraborty, and S. M. Shivaprasad, J. Vac. Sci. Technol. A **6**, 3120 (1988).